scientific reports

Check for updates

OPEN

A head-to-head comparison of polymer interaction with mucin from porcine stomach and bovine submaxillary glands

Mai Bay Stie[1,2]✉, Cristiana Cunha[1,2], Zheng Huang[1,2], Jacob Judas Kain Kirkensgaard[3,4], Pernille Sønderby Tuelung[5], Feng Wan[1,2], Hanne Mørck Nielsen[1,2], Vito Foderà[1,2] & Stine Rønholt[6]✉

Native mucus is heterogeneous, displays high inter-individual variation and is prone to changes during harvesting and storage. To overcome the lack of reproducibility and availability of native mucus, commercially available purified mucins, porcine gastric mucin (PGM) and mucin from bovine submaxillary gland (BSM), have been widely used. However, the question is to which extent the choice of mucin matters in studies of their interaction with polymers as their composition, structure and hence physicochemical properties differ. Accordingly, the interactions between PGM or BSM with two widely used polymers in drug delivery, polyethylene oxide and chitosan, was studied with orthogonal methods: turbidity, dynamic light scattering, and quartz crystal microbalance with dissipation monitoring. Polymer binding and adsorption to the two commercially available and purified mucins, PGM and BSM, is different depending on the mucin type. PEO, known to interact weakly with mucin, only displayed limited interaction with both mucins as confirmed by all employed methods. In contrast, chitosan was able to bind to both PGM and BSM. Interestingly, the results suggest that chitosan interacts with BSM to a greater extent than with PGM indicating that the choice of mucin, PGM or BSM, can affect the outcome of studies of mucin interactions with polymers.

Keywords Mucin, PGM, BSM, Polymer, Chitosan, QCM-D

Drug delivery via mucosal surfaces has high patient acceptance and holds the potential to improve the efficiency of numerous drugs. However, mucus, the viscoelastic gel that lubricates all mucosae, can constitute a significant steric and interactive barrier hindering optimal drug delivery. In addition, mucus shedding leads to short retention times of drug at the mucosal surface and thus a loss of drug available for absorption[1]. An approach to improve drug delivery limited by the presence of mucus is thus to improve drug diffusion through the mucus and, in general, to minimize the impact of the mucus barrier[1]. Also, improving adhesion to mucosal surfaces can be an effective strategy for local treatment or to improve systemic drug absorption by maintaining a high concentration of drug at the site of absorption for a longer period[2]. Accordingly, it is of great interest to evaluate the potential interaction of drugs, excipients, and drug delivery systems with mucus at the dosing site.

Native mucus is heterogeneous, displays high inter-individual variation, and can be prone to changes during harvesting and storage, and its availability may be limited[3]. Therefore, studies with native mucus are in general challenged by large deviations and lack of reproducibility, which can make it difficult to clarify the specific mechanisms responsible for the interaction of excipients, drugs, and drug delivery systems with mucus[4]. Instead, mechanistic studies based on biophysical methods are often used with mucins purified from mucus isolated from animal or man. Although, these large glycoproteins only make up 1–5% of the content of mucus, the network

[1]Department of Pharmacy, University of Copenhagen, Universitetsparken 2, 2100 Copenhagen, Denmark. [2]Center for Biopharmaceuticals and Biobarriers in Drug Delivery (BioDelivery), University of Copenhagen, Universitetsparken 2, 2100 Copenhagen, Denmark. [3]Department of Food Science, Rolighedsvej 26, 1958 Frederiksberg, Denmark. [4]Niels Bohr Institute, Universitetsparken 5, 2100 Copenhagen, Denmark. [5]Department of Drug Design and Pharmacology, Faculty of Health and Medical Sciences, University of Copenhagen, Universitetsparken 2, 2100 Copenhagen, Denmark. [6]LEO Foundation Center for Cutaneous Drug Delivery, University of Copenhagen, Universitetsparken 2, 2100 Copenhagen, Denmark. ✉email: mai.bay.stie@sund.ku.dk; stine.roenholt@sund.ku.dk

of mucins is the main steric and interactive barrier of mucus, and it dictates many of its properties such as the viscoelasticity and the negative charged state of mucus; both important for its interaction with drug delivery systems and their components[1,5]. Employing purified mucins instead of native mucus in mechanistic studies provides better sample reproducibility and allows for a higher degree of control of the sample properties and its individual components[4].

Mucins are secreted and membrane-bound to mucosae giving rise to distinct groups of mucins[1]. Mucins have been purified from different anatomical sites and from different species. Consequently, depending on their origin, they display different molecular properties, although some overlap exists[1,4,6]. For example, the human *MUC5AC* gene that encodes for the major gel-forming mucin of the stomach, MUC5AC, is a homolog of the porcine gastric mucin (PGM) gene[7,8]. MUC5AC is also expressed in mucus of the respiratory tract[9] and eyes[10]. Similarly, bovine submaxillary gland mucin (BSM) is rich in the translational product of the *BSM* gene; a potential homolog to the human h*MUC19*, which encodes the gel forming mucin expressed in human salivary glands[11]. In addition, the same gene-product can have different patterns of glycosylation, depending on anatomical location and type of species that likely affect the function of the mucin[12]. To the best of our knowledge, only two purified mucins are commercially available, namely porcine gastric mucin (PGM) and bovine submaxillary gland mucin (BSM). Especially PGM is widely used in research, mainly because of its greater availability and lower price than for BSM: the cost of BSM is several 100-fold higher than PGM (both provided by Sigma-Aldrich, St. Louis, MO, USA). By using commercially available mucins, comparisons can easier be made across studies performed by different research groups. However, the question is to which extent the choice of mucin type matters as their properties varies. PGM has been used to simulate mucus from the gastro-intestinal tract[3], but also other anatomical sites including the respiratory tract[13] and the oral cavity[14,15]. Likewise, use of BSM has not only been restricted to modelling the mucus of the oral cavity[16], but also, for example, the respiratory tract[17]. Overall, the choice of commercial mucin used may be based on availability as much as anatomical origin and often no criteria are given to justify the choice of a specific commercial mucin. This likely poses a significant concern, as differences in mucin composition between PGM and BSM could influence the study outcomes. For example, according to the manufacturer's (Sigma-Aldrich, St. Louis, MO, USA) information, PGM contains significantly less bound sialic acid (Type II: ≤ 1.2%, Type III: 0.5–1.5%) in contrast to BSM (9–24%). The difference in content of sialic acid in BSM compared to PGM has also been confirmed experimentally[18]. In general, mucins purified from different anatomical sites (i.e., stomach versus submaxillary glands) and species (i.e., from porcine versus bovine) naturally contain different types of mucins, and consequently will display different properties. In addition, the method of purification and level of impurities might affect the physicochemical properties of the mucin test sample dispersion.

We hypothesize that differences in mucin composition, specifically in PGM versus BSM, will affect the interaction of excipients with mucins. Accordingly, the interactions between mucin and two widely used polymers in drug delivery, polyethylene oxide (PEO) and chitosan, were investigated because of their known differences in degree of mucoadhesion. Chitosan is positively charged under acidic conditions and interacts with the negatively charged mucins through a combination of ionic interactions and hydrophobic interactions[19], whereas PEO is a synthetic polymer with a neutral charge that only binds weakly to mucin[20]. We specifically compare the interaction of PEO and chitosan with commercially available mucins from two anatomical origins, PGM and BSM, using in vitro orthogonal physicochemical methods frequently used to assess mucoadhesion.

Results and discussion

A larger fraction of BSM than of PGM interacts with chitosan

Commercial PGM and BSM were obtained as powders; PGM appeared compact and yellow, whereas BSM appeared fluffy and white (Fig. 1A). Differences in appearance might not only be related to the composition of the mucins but also to the procedure of drying after preparation of the mucin. In the present work, the same concentrations (w/v) of PGM and BSM suspended in water were characterized by recording their respective absorbances and circular dichroism (CD) spectra, and the results revealed clear differences between the two types of mucins. PGM displayed a significantly higher absorbance at 280 nm (tyrosine and tryptophan absorbance) as compared to BSM that only displayed very limited absorbance at the same nominal concentration (0.8 mg/mL) (Fig. 1B). In addition, the absorbance spectrum of PGM revealed a significant contribution from light scattering at higher wavelengths due to the turbid appearance of this mucin suspension (Fig. 1B). The secondary structure of both free mucins, PGM and BSM, in ultrapure water was investigated by CD spectroscopy. Spectra of PGM and BSM have ellipticity minima that are typical for a random coil conformation; the minima for the PGM spectra being at a slightly lower wavelength (196 nm) than for BSM (202 nm) (Fig. 1C) in accordance with the finding of others[21]. In general, because of the high complexity of mucins, they are often described by the bottle brush model fitting small-angle X-ray scattering (SAXS) data[22]. Mucin consists of a long protein chain with segments of highly glycosylated and densely packed oligosaccharide side chains, thus resembling a bottle brush. SAXS curves presented in Fig. 1D indicate that PGM and BSM have different features around q = 0.1–1 Å (Fig. 1D). The SAXS curve of PGM is in accordance with the data for the lowest mucin concentration evaluated by Falk et al.[22], where extensive data modeling was performed assuming a bottle brush structure of this mucin. BSM does not show the same form factor scattering as PGM but displays the swollen chain power law scaling[23] with a slope of approximately -1.62, suggesting that the structure of the bottlebrush for BSM shows the signature of a swollen linear polymer (Fig. 1D). In general, the results underline the fact that PGM and BSM have different compositions e.g., amino acid sequence and sialic acid content[18], and different features that could affect the study outcome based on which mucin is chosen.

Turbidity measurements can be used to evaluate the mucoadhesive properties of polymers, and, to some extent, rank polymers based on their degree of mucin binding[24–26]. When hydrated, PGM formed a turbid

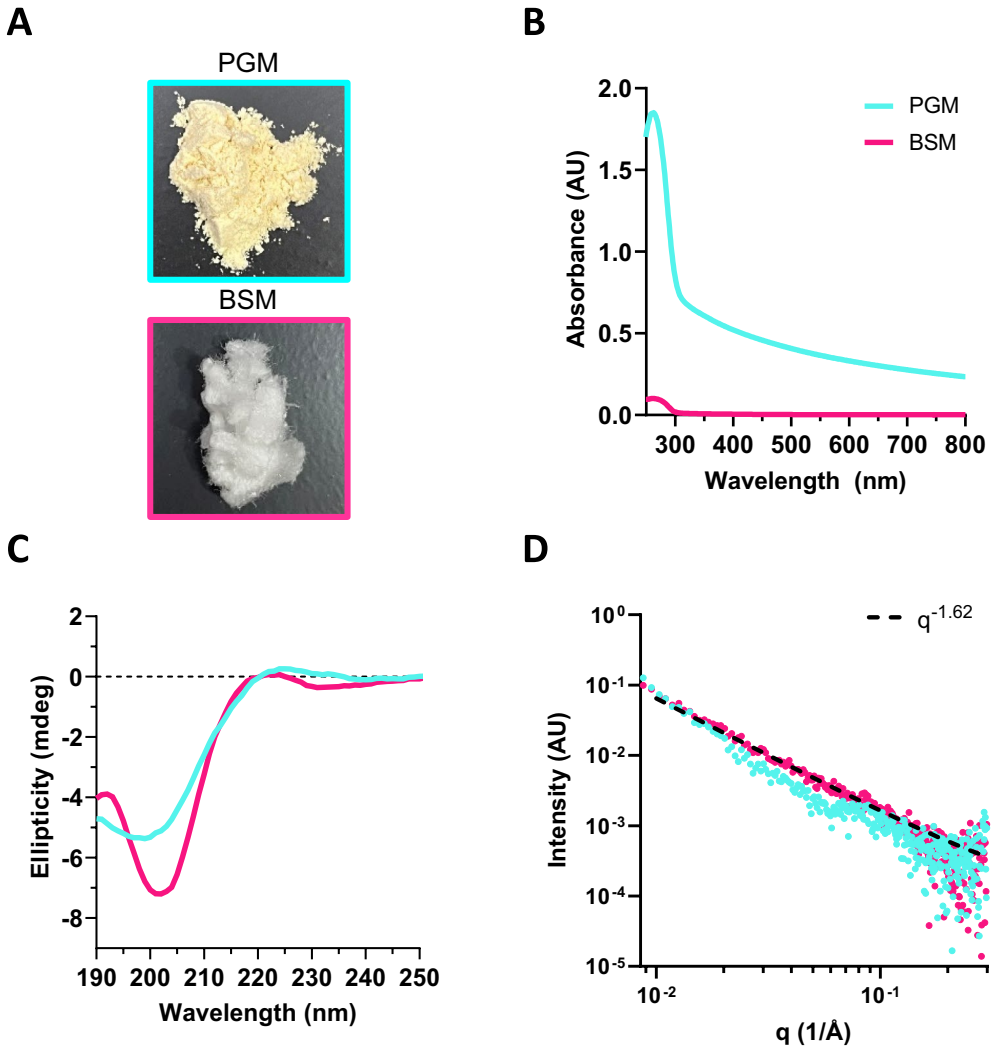

Fig. 1. Characterization of commercially available mucins, PGM (turquoise) and BSM (pink). (**A**) Images of mucin powder: PGM (compact and yellow, top) and BSM (fluffy and white, bottom). (**B**) Representative absorbance spectra of 0.8 mg/mL mucin, PGM and BSM, in water. N = 2. (**C**) Representative CD spectra of 0.2 mg/mL PGM and BSM in water. N = 2, n = 3. (**D**) Representative small-angle X-ray scattering curves of 0.8 mg/mL PGM and BSM in water. N = 2. In general, N represents the number of individual samples prepared on different days, and n represents the number of scans per sample.

suspension; in contrast, BSM was transparent at the same w/v concentration (Fig. 2A). This is in accordance with the findings of others. For example, Klemetsrud et al.[27], studied suspensions of PGM and BSM by atomic force microscopy (AFM) and found PGM to be a turbid suspension with a particulate structure; in contrast to BSM that gave a clear sample and showed an outstretched structure of the mucin by AFM. PEO and chitosan dispersions appeared transparent at the concentrations used. No increase in turbidity was observed after mixing PEO with PGM nor BSM, thus showing the limited binding of PEO to either of the mucins, as expected for this negative control (Fig. 2B). In contrast, mixing chitosan with PGM or BSM resulted in a high increase in turbidity (Fig. 2B). The increase in turbidity due to complexation of PGM with chitosan was approximately two-fold (Fig. 2B), and the turbidity increase was significantly higher for mixtures of chitosan with BSM compared to PGM. In this experiment, the ratio between chitosan and mucin was fixed, and the results thus suggest that chitosan binds to BSM to a greater extent than to PGM.

Interaction of polymer with mucin can result in the formation of large complexes/aggregates as demonstrated (Fig. 2A), and these can be removed by centrifugation. Accordingly, clear solutions (supernatant) were obtained for all samples after centrifugation. By the colorimetric BCA assay, the mucin concentration in the supernatant after centrifugation was determined for mucin samples mixed with polymer and related to the mucin concentration of neat mucin, PGM or BSM, after centrifugation. In general, no detectable change in protein concentration was observed for mucins, PGM or BSM, mixed with PEO, as expected (Fig. 2C). Also, no detectable change in protein concentration in the supernatant was observed for PGM mixed with chitosan (Fig. 2C). This is surprising, as the turbidity measurements suggested an interaction between chitosan and PGM indicated by an increase in turbidity. The results could indicate that only a small fraction of the PGM interacted with chitosan or that

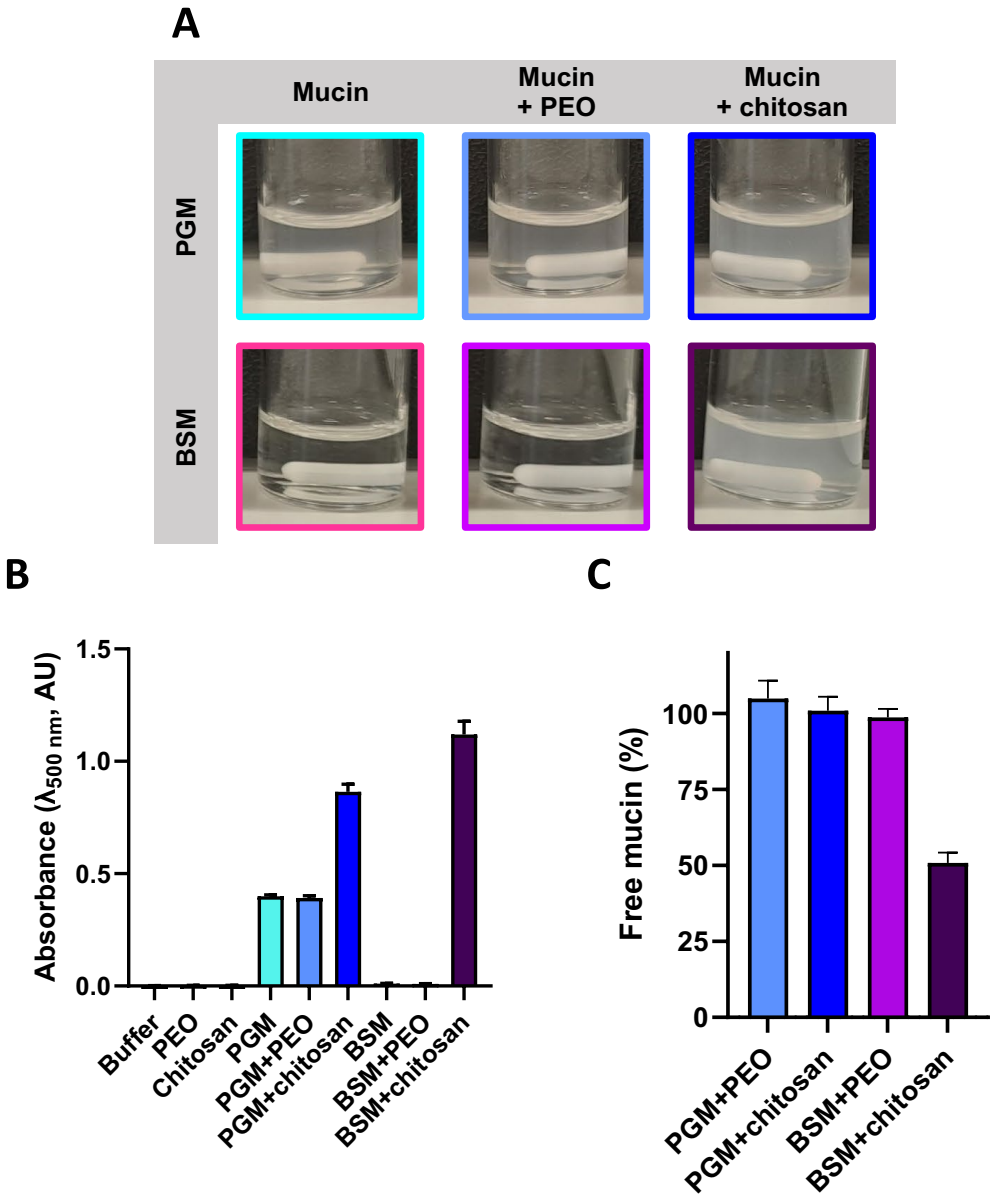

Fig. 2. Interaction of PEO and chitosan with PGM (turquoise/blue) or BSM (pink/purple) evaluated by turbidity measurements. (**A**) Images of neat mucin, PGM or BSM, or mucins mixed with PEO and chitosan. (**B**) Turbidity measurements of samples in buffer, PEO, chitosan, PGM, BSM and mucins (PGM/BSM) mixed with PEO or chitosan. The absorbance contribution from buffer, PEO, chitosan, BSM and BSM + PEO was below the limit of detection. (**C**) Protein content in mucin samples (PGM or BSM) remaining after mixing with polymer (PEO or chitosan) and subsequent centrifugation (free mucin). Data are relative to the concentration of centrifuged neat mucin. Results presented as mean + standard deviation. N = 3, where N represents the number of individual samples prepared on different days.

the bound fraction was not easily detected by the BCA assay (yet induced a measurable turbidity increase). In contrast, ~ 50% of the protein concentration of BSM interacted with chitosan to form larger mucin-polymer complexes as determined by the BCA assay (Fig. 2C). This could suggest that chitosan interacted very strongly with a significant fraction of BSM, forming complexes that were dense and big enough to be removed by centrifugation. Furthermore, PGM and BSM have been shown to contain aggregates and contaminants such as albumin that could affect the results[18,28]. In addition, batch-to-batch variation has been reported[18]. In general, such contaminants are thought to bring additional functions to the mucins in vivo, which is a subject still under investigation. Here, a single batch of PGM or BSM was used in the studies, and the mucins were used as received.

PGM and BSM display different particle size distributions both before and after interacting with PEO and chitosan

Analysis of turbidity can be coupled with other methods such as DLS to measure the size distributions of mucins and of the mucin-polymer complexes formed in bulk (Fig. 3, Table 1). Both PGM and BSM showed very polydisperse particle populations with PDI > 0.5 (Table 1). For PGM, the particle size distribution based on intensity was dominated by a single peak representing particles with a diameter of ~ 900 nm (Fig. 3A). The solution of PGM is turbid suggesting the presence of large particles. The size estimates of PGM by DLS could thus be overpowered by the presence of large species (a well-known artifact of DLS) as the scattering intensity is proportional to the 6th power of the diameter of the particles. The presence of undetected smaller species in the PGM sample cannot thus be ruled out. In contrast, BSM displayed a bimodal size distribution with a particle diameter spanning from ~ 20 nm to several hundred nanometers (Fig. 3B). Mixing PGM with PEO induced a small shift in particle size but with no concurrent change in PDI (Fig. 4A, Table 1). No significant difference in the size distribution of BSM was observed after mixing with PEO (Fig. 3B, Table 1). This was in accordance with the turbidity measurements, suggesting that PEO only bound weakly to mucin independently of the mucin type (Fig. 2). Interaction of chitosan with PGM induced an increase of the Z-average and a decrease in PDI showing association of chitosan with the mucin (Fig. 3A, Table 1). Interestingly, the effect of chitosan binding to BSM induced a more prominent change in the size distribution profile, as mixing BSM with chitosan resulted in the formation of a monodisperse (PDI of 0.05 ± 0.03, Table 1) particle population with a significant increase in the average particle size diameter. This suggests a difference in the interaction of chitosan with BSM as compared to PGM; in accordance with the turbidity measurements (Fig. 2).

In general, suspensions of mucin display large heterogeneity, which can make it difficult to decipher the level of interaction with polymers. Sonication of the mucin (PGM) suspension has been attempted by Albarkah et al.[29], to obtain a more homogeneous size distribution of mucin particles. That resulted in a narrower size distribution, but the effect was only temporary as some smaller species obtained by sonication gradually reassembled to form larger agglomerates[29]. An alternative and commonly used method is separating the mucin suspension into different fractions by centrifugation and/or filtering[20]. By this, a more homogeneous sample of mucin will be obtained but it might result in loss of fractions that are of importance for the interaction with e.g., polymers as well as intermolecular mucin-mucin interactions.

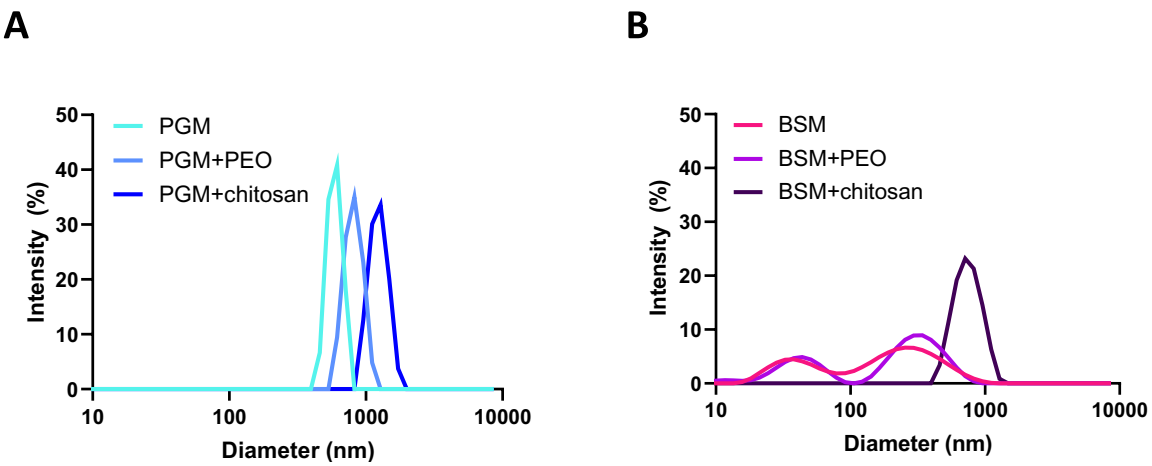

Fig. 3. Particle size distribution by intensity of mucins, PGM (turquoise/blue) or BSM (pink/purple), and after mucin interacting with PEO and chitosan. (**A**) Neat PGM and PGM mixed with PEO or chitosan. (**B**) Neat BSM and BSM mixed with PEO or chitosan. Representative curves. N = 2, n = 1–2, where N represents the number of mucin suspensions evaluated on different days, and n is the number of technical sample replicates, giving ≥ 3 measurements per sample.

	Z-average (nm)		PDI	
	PGM	BSM	PGM	BSM
Mucin	992 ± 123	87 ± 3	0.52 ± 0.05	0.57 ± 0.02
Mucin + PEO	1352 ± 111	95 ± 3	0.48 ± 0.13	0.60 ± 0.09
Mucin + chitosan	1768 ± 271	645 ± 42	0.31 ± 0.10	0.05 ± 0.03

Table 1. Z-average and polydispersity index (PDI) of samples of neat mucins, PGM or BSM, and upon interacting with PEO or chitosan. Results presented as mean ± standard deviation. N = 2, n = 1–2, where N represents the number of mucin suspensions evaluated, and n is the number of technical sample replicates, giving ≥ 3 measurements per sample.

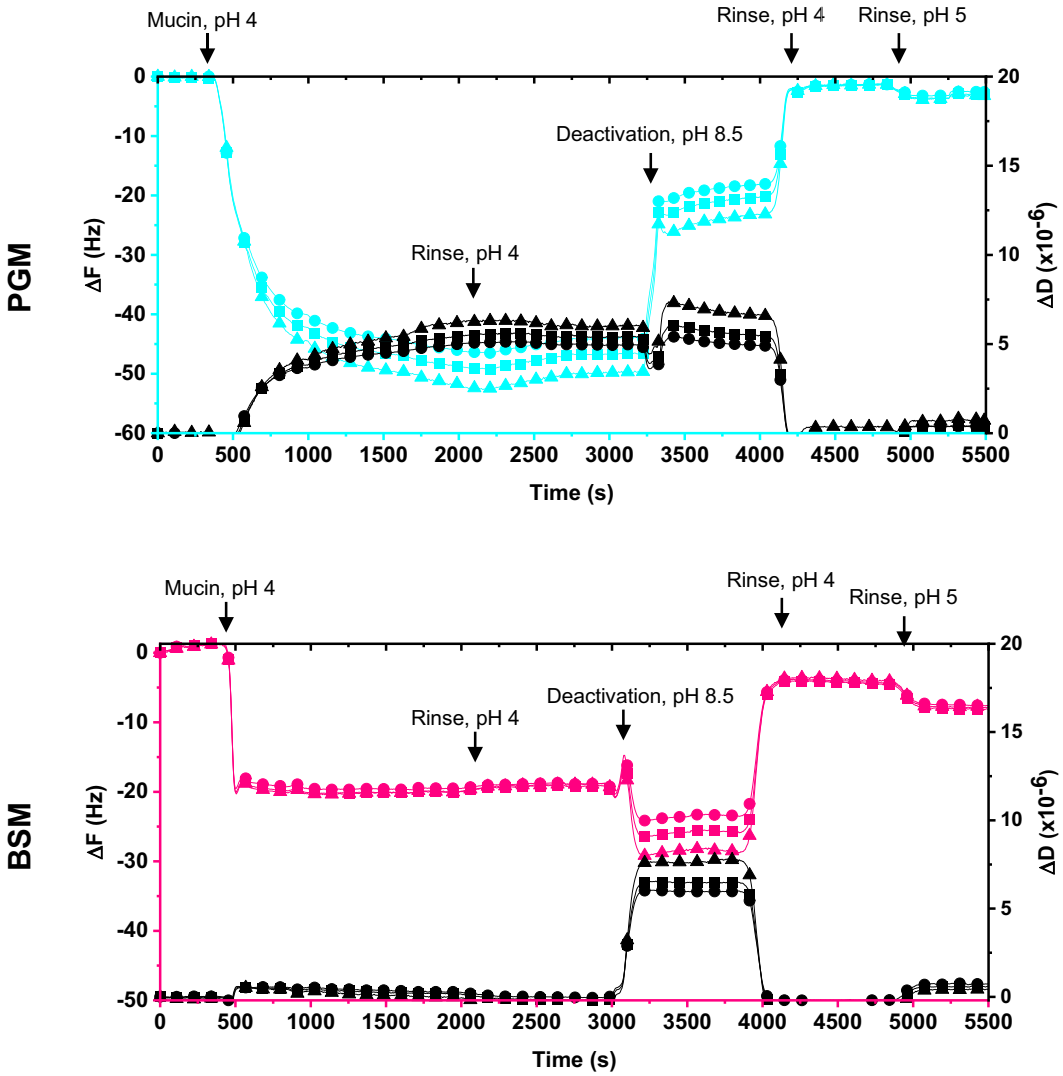

Fig. 4. Representative QCM-D measurement of changes in frequency (ΔF, turquoise/pink) and dissipation (ΔD, black) during the adsorption of mucin onto the QCM-D sensor achieved by NHS functionalization. Top: PGM; bottom: BSM. The fifth (circles), seventh (squares) and ninth (triangle) overtones are shown. N ≥ 2, n = 4, where N represents the number of individual mucin samples prepared on different days, and n is the number of technical repeats per mucin sample.

Polymer interaction with immobilized mucin monitored by QCM-D depends on mucin type

Quartz crystal microbalance with dissipation monitoring (QCM-D) is a valuable technique to monitor interactions in real time. The turbidity evaluated by spectrophotometry and the particle size evaluated by DLS of the mucin samples with polymers were evaluated after 30 min of incubation. In contrast, mucin-polymer interaction can be evaluated in real time at a time scale of seconds by QCM-D. This method has been used to evaluate the interaction of various polymers with mucin, including chitosan[16,30] but also interactions of particulate drug delivery systems with mucin, e.g., for pulmonary drug delivery[13]. Changes in the absorbed mass e.g., mucin or polymer on the sensor are proportional to changes in the frequency (ΔF). Information on the viscoelastic properties of the adsorbed layer is given by the changes in dissipation (ΔD) and spreading of the overtones. Firstly, mucin, PGM or BSM, was chemically immobilized on the gold quartz sensor by NHS-functionalization, as we previously found that this method was suitable for establishing a stable layer of BSM to study the interaction with chitosan[16]. The respective ΔF and ΔD curves for PGM and BSM were significantly different during mucin immobilization (Fig. 4). The initial adsorption of BSM to the sensor was significantly faster compared to that of PGM seen by that the QCM-D curve for BSM showed a much faster change (steeper slope) in ΔF over time and reached a plateau significantly faster than that for PGM. Also, spreading of overtones during the initial adsorption of mucin was more prominent for PGM compared to BSM, indicative of the formation of a more viscoelastic mucin layer. Rinsing did not induce a significant change in ΔF for neither of the mucins confirming the formation of a mucin layer on the sensor. Subsequently, deactivation at pH 8 and rinsing first at pH 4 and then pH 5 affected the properties of the layer of PGM and BSM differently. Although multiple factors might play a role during the process of functionalization of the sensor, this observation could suggest that the mucins, PGM and

BSM, display different behaviors depending on pH. This is an interesting observation in the light of the fact that PGM and BSM originate from two anatomical sides with vastly different pH environments, being predominantly acidic for the stomach (PGM) and close to neutral for the oral cavity (BSM), and because the mucins are used to model different anatomical sites often not considering the effect of the pH environment on the mucin structure and function. The process followed by rinsing resulted in a stepwise decrease in ΔF for PGM, indicative of loss of water bound in the layer and the formation of a very rigid PGM layer on the sensor (low ΔF and ΔD, no spreading of overtones) and/or significant loss of mucin during this part of the process. The results could also suggest that only a limited amount of PGM and/or contaminants was bound to the sensor after the final rinse due to the low ΔF. In contrast, deactivation of the formed BSM layer at pH 8 resulted in a more viscoelastic (increase ΔD, spreading of overtones) and more hydrated (decrease in ΔF) mucin layer, as previously shown[16,31]. The final mucin layer after rinsing at pH 4 and then pH 5 also resulted in a rigid BSM layer on the sensor (low ΔF and ΔD, no spreading of overtones). Differences in the behavior of the PGM and BSM layer during functionalization of the sensor might be ascribed to differences in the properties of the two mucins depending on pH[21], differences in mucin composition, and/or water within the mucin layer during the deactivation process. This could all affect the availability of the mucin molecules to interact with the polymers as was investigated next.

In general, the association of PEO with the mucin layers showed the same trend regardless of mucin origin, PGM or BSM: a decrease in ΔF and increase in ΔD concomitant with introduction of PEO indicating adsorption of PEO to both mucin types (Fig. 5). A slightly lower decrease in ΔF and higher increase in ΔD were seen for the association of PEO with BSM compared to PGM. Regardless of the mucin type, the interaction of PEO was, as expected, weak and reversible as rinsing resulted in a change in ΔF towards less negative values indicative of a significant loss of mass, i.e., PEO. Chitosan also showed only limited adsorption to the layer of PGM, and rinsing resulted in a change in ΔF towards the starting value suggesting loss of chitosan, i.e., reversible adsorption to PGM (Fig. 5, top). In contrast, as previously shown[16], chitosan displayed strong adsorption to BSM and rinsing had limited effect on the ΔF and ΔD, indicative of stable complex formation between chitosan and BSM (Fig. 5, bottom). Looser adsorption of chitosan to the PGM compared to BSM may not only be attributed to differences in mucin type but could also be affected by differences in the layers formed on the QCM-D sensor as mentioned above (Fig. 4). By using the presented method of QCM-D, BSM showed better performance compared to PGM according to the predictability of PEO and chitosan adsorption to a mucin layer. Moreover, Oh et al.[30], found that the interaction of chitosan with mucin purified from native porcine gastric mucus was very different from

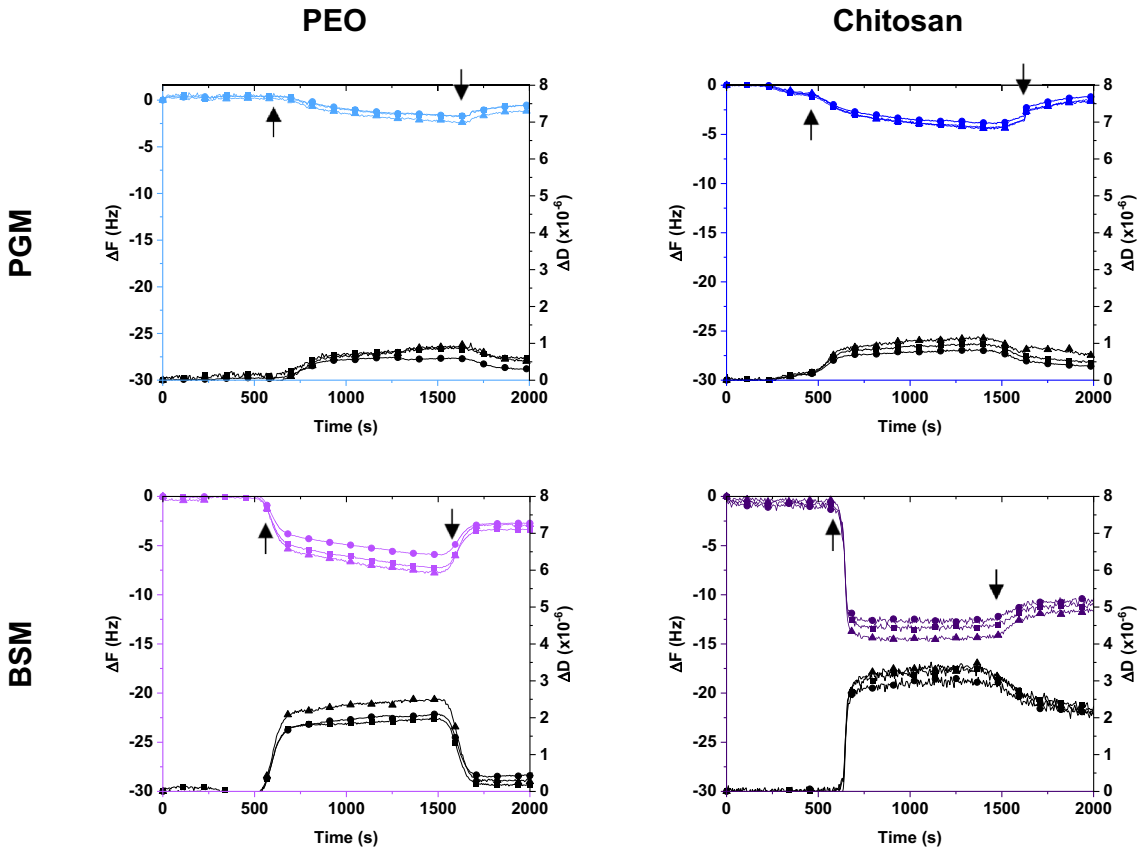

Fig. 5. Representative QCM-D measurements of changes in frequency (ΔF, blue/purple) and dissipation (ΔD, black) after exposing the established mucin layer to PEO or chitosan. Top: PGM; bottom: BSM. The fifth (circles), seventh (squares) and ninth (triangle) overtones are shown. The first arrow indicates introduction of polymer, and second arrow indicates rinsing of the mucin layer with acetate buffer pH 5. N ≥ 2, n = 2, where N represents the number of individual mucin samples and n is the number of repeats per sample.

commercial PGM[28]. In other studies, Lundin et al.[28], and Feiler et al.[32], investigated the film-forming properties of BSM as received and after further purification by using e.g. QCM-D. Although, BSM adsorbed quantitatively in the same way independent of the degree of purity in the study, the presence of an increasing amount of BSA, resulted in the formation of thicker and more rigid films[28,32]. This highlights the fact that not only mucin composition, but also the method and extent of mucin purification and thus the presence of other constituents can affect the study outcome[28].

Conclusion

Mucins are not only the main constituents of secreted mucus but also exists bound to mucosal tissue, and their properties and presence are important in drug delivery. By using absorption spectroscopy, CD, and SAXS, this study reveals that PGM and BSM are physically and structurally different. Furthermore, complementary methods (turbidity and DLS) were used to study binding of pharmaceutically relevant polymers to the two different mucins in solution, and QCM-D was employed to study adsorption of the polymers to mucins tethered to a surface. We show that polymer binding and adsorption to the two commercially available mucins, PGM and BSM, are different depending on the mucin type as well as depending on the polymer type. PEO is known to interact weakly with mucin, and as expected only displayed limited interaction with both mucin types as confirmed by all methods employed. In contrast, chitosan bound to both PGM and BSM, and interestingly, results from both DLS measurements, turbidity measurement with determination of free mucin, and QCM-D could suggest that chitosan interacts with BSM to a greater extent than with PGM. More studies are, however, needed to better understand the underlying cause for the observed difference in interaction depending on mucin type. An increasing number of studies suggests that mucin purified in a laboratory scale benefits from higher native resemblance as compared to commercial mucins[4]. Nevertheless, the broad usability of commercially available mucins in many different research fields and better reproducibility across different research groups favor the continuous use of these. With this interdisciplinary work, novel insight was provided to highlight how the choice of mucin can impact the outcome of mucin interaction studies of relevance for the development of drug delivery systems targeting mucosal surfaces.

Materials and methods

Materials

Chitoceuticals chitosan 95/100 (DDA 96%, Mw 100–250 kDa) was purchased from Heppe Medical Chitosan (Halle, Germany). Mucin from porcine stomach (Type II), mucin from bovine submaxillary glands (Type I-S), PEO (Mw ~900 kDa), bovine serum albumin (BSA), acetic acid, Tris, *N*-(3-dimethylaminopropyl)-*N*′-ethylcarbodiimide hydrochloride (EDC), *N*-hydroxysuccinimide (NHS), ethanolamine hydrochloride (ETA-HCl) and 11-mercaptoundecanoicacid (MUA) were obtained from Sigma Aldrich (St. Louis, MO, USA). Pierce™ BCA Protein Assay Kit was obtained from Thermo Fisher Scientific (Waltham, MA, USA). Ethanol (absolute) and sodium hydroxide were purchased from VWR (Søborg, Denmark). Pierce™ BCA protein assay kit for protein determination was purchased from Thermo Fisher Scientific (Roskilde, Denmark). Ultrapure water (18.2 MΩ × cm) purified by a PURELAB flex 4 (ELGA LabWater, High Wycombe, UK) was used.

Circular dichroism (CD) spectroscopy

Mucin, either BSM or PGM, was used as received and hydrated in ultrapure water to a final concentration of 4 mg/mL and stirred at mild speed overnight at 4 °C. Mucin in water will be described as suspension as they also contain an insoluble fraction. On the day of the experiment, the mucin suspensions were stirred at room temperature (RT). The mucin suspensions were then centrifuged for 15 min at 10,000 rpm (9279×*g*) at 25 °C and diluted to 0.2 mg/mL in ultrapure water. CD measurements were acquired in the far-UV region (190–250 nm, step size of 1 nm) using a Chirascan CD spectrometer (Applied Photophysics, Leatherhead, UK). A quartz cuvette with 1 mm path length (Hellma Analytics, Müllheim, Germany) was used, and the spectra were collected at 25 °C with a scan speed of 0.5 s per step and 1 nm bandwidth. To obtain the ellipticity, 3 scans were recorded for each sample, and the background signal was automatically subtracted. The data were corrected for the blank (ultrapure water) and normalized to the baseline (subtracting the CD signal at 250 nm). The ellipticity curves of each mucin were smoothed using a second order smoothing polynomial (5-point) Savitzky-Golay method on GraphPad Prism (version 9.5.1).

Small-angle X-ray scattering (SAXS)

Mucin, either BSM or PGM, was used as received and hydrated in ultrapure water to a final concentration of 4 mg/mL and stirred at mild speed overnight at 4 °C. On the day of experiment, the mucin suspensions were stirred at RT. The mucin suspensions were diluted to 0.8 mg/mL with 0.5% (v/v) acetate pH 5. For the small angle X-ray scattering experiments, a BioXolver L (Xenocs, Grenoble, France) equipped with a liquid gallium X-ray source was used and a wavelength of $\lambda = 1.34$ Å. Here $|q| = 4\pi\lambda \sin(\theta)$, is the length of the scattering vector, 2θ is the scattering angle, and λ the wavelength. An automated sample loading system was used, and a sample exposure of 10 frames × 60 s (SD = 632.5) or 30 frames × 60 s (SD = 1057.5) at RT. BIOXTAS RAW (Version 2.1.1) was used for radial averaging of the 2D images and primary data reduction[33]. All frames were averaged, and the corresponding averaged buffer subtracted.

Spectrophotometry

3 mg of chitosan or PEO was dispersed in 28 mL ultrapure water and 150 µL acetic acid (glacial) was added. The polymer dispersions were stirred overnight at RT to ensure complete hydration of the polymers. 1 M NaOH was added to reach a pH of 5 and ultrapure water was added to a final volume of 30 mL giving a polymer

concentration of 0.1 mg/mL. Mucin, either BSM or PGM, was used as received and hydrated in ultrapure water to a final concentration of 4 mg/mL, and stirred at mild speed overnight at 4 °C. On the day of experiment, the mucin suspensions were allowed to equilibrate to RT under mild stirring. 400 µL mucin suspension was added to 1.6 mL polymer dispersion, chitosan or PEO, and stirred for 30 min at RT. Mucin mixed with 0.5% (v/v) acetate pH 5 was used as a control. As a measure of turbidity, the absorbance was hereafter measured at 500 nm on a UV-1900 spectrophotometer in a quartz cuvette with a path length of 1 cm at RT (Shimadzu, Ballerup, Denmark).

Bicinchoninic acid (BCA) assay

Samples prepared for the turbidity measurements were stored frozen, hereafter thawed, and centrifuged at 10,000 rpm (9279×*g*) for 10 min at 25 °C. The concentration of mucin, PGM or BSM, in the supernatant after mixing with PEO or chitosan was determined relative to the mucins alone. BSA was used as reference protein for the standard curve (23.4—500 µg/mL, $R^2 \geq 0.99$). Shortly, a volume of 25 µL of the supernatant was transferred to a clear flat bottom polystyrene 96-well microplate (Greiner Bio-One, Kremsmünster, Austria) incubated with 200 µL of BCA working reagent at 37 °C for 30 min. The absorbance of the samples was then measured at 562 nm in a plate reader (POLARstar OPTIMA, BMG LABTECH, Ortenberg, Germany). The relative amount of free mucin (%) in the supernatant was calculated based on the mucin concentration (c) in samples with mucin alone and when mixed with polymer by using a standard curve and calculated according to Eq. (1).

$$\text{Free mucin (\%)} = 100\% - \left(\frac{c_{\text{mucin}} - c_{\text{mucin+polymer}}}{c_{\text{mucin}}} \cdot 100\% \right) \quad (1)$$

Dynamic light scattering (DLS)

Based on DLS, the average size and polydispersity index (PDI) were measured at 25 °C in a UV microcuvette with 10 mm path length using a Zetasizer Nano ZS (Malvern Instruments, Worcestershire, UK) equipped with a 633 nm laser and 173° detection optics. Malvern DTS v.6.20 software was used for data acquisition and analysis. The sample was allowed to equilibrate for 60 s before starting the measurement. For each sample, three measurements were performed, and the average used as the readout.

Quartz crystal microbalance with dissipation monitoring (QCM-D)

The experiment was conducted according to Stie et al.[16]. In short, 0.5 mg/mL mucin, BSM or PGM, in 10 mM acetate pH 4 was prepared and stored at 4 °C overnight. 0.2 mg/mL chitosan or PEO was dispersed in 0.5% (v/v) acetate buffer pH 5 and stirred overnight at RT. The gold-coated quartz crystals were incubated with 1 mM MUA in ethanol for 12 h at RT, hereafter rinsed in ethanol and dried. On a E4 Q-sense (Bioline Scientific, Gothenburg, Sweden), the sensors were flushed with to 200 mM EDC and 50 mM NHS and rinsed in ultrapure water and hereafter in 10 mM acetate pH 4. The sensors were then flushed with 0.5 mg/mL mucin, PGM or BSM, in acetate pH 4 for 30 min and hereafter rinsed with 10 mM acetate pH 4.0 for 30 min. Then, the sensors were exposed to 1 M ETA-HCl in 10 mM Tris buffer pH 8.5 for 30 min, followed by two cycles of rinsing; the first one in 10 mM acetate buffer pH 4.0 for 15 min and then one in 0.5% (v/v) acetate buffer pH 5.0 for 15 min. The mucin layer on the sensors was exposed to 0.2 mg/mL chitosan or PEO in 0.5% (v/v) acetate buffer pH 5.0 for 15 min. Finally, the sensors were rinsed for 15 min in 0.5% (v/v) acetate buffer pH 5.0. The flow rate was 50 µL/min, and the experiments were run at 37 °C. Changes in frequency (ΔF) and energy dissipation factor (ΔD) were recorded simultaneously for the fifth, seventh and ninth overtones.

Data availability

The datasets generated during and/or analyzed during the current study are available from the corresponding author on reasonable request.

Received: 31 May 2024; Accepted: 4 September 2024
Published online: 12 September 2024

References

1. Mortensen, J. S., Stie, M. B., Harloff-Helleberg, S. & Nielsen, H. M. Overcoming the mucus barrier. In *Organelle and Molecular Targeting*. 355–380 (2021).
2. Peppas, N. A., Thomas, J. B. & McGinty, J. Molecular aspects of mucoadhesive carrier development for drug delivery and improved absorption. *J. Biomater. Sci. Polym. Ed.* **20**, 1–20 (2009).
3. Boegh, M., Baldursdóttir, S. G., Müllertz, A. & Nielsen, H. M. Property profiling of biosimilar mucus in a novel mucus-containing in vitro model for assessment of intestinal drug absorption. *Eur. J. Pharmaceut. Biopharmaceut.* **87**, 227–235 (2014).
4. Marczynski, M., Kimna, C. & Lieleg, O. Purified mucins in drug delivery research. *Adv. Drug Deliv. Rev.* **178**, 113845 (2021).
5. Bansil, R. & Turner, B. S. The biology of mucus: Composition, synthesis and organization. *Adv. Drug Deliv. Rev.* **124**, 3–15 (2018).
6. Mackie, A. R. *et al.* Innovative methods and applications in mucoadhesion research. *Macromol. Biosci.* **17**, 1600534 (2017).
7. Turner, B. S., Bhaskar, K. R., Hadzopoulou-Cladaras, M. & LaMont, J. T. Cysteine-rich regions of pig gastric mucin contain von Willebrand factor and cystine knot domains at the carboxyl terminal. *Biochim. Biophys. Acta (BBA) - Gene Struct. Exp.* **1447**, 77–92 (1999).
8. Celli, J. P. *et al.* Rheology of gastric mucin exhibits a pH-dependent sol–gel transition. *Biomacromolecules* **8**, 1580–1586 (2007).
9. Lillehoj, E. P., Kato, K., Lu, W. & Kim, K. C. *Cellular and Molecular Biology of Airway Mucins*. 139–202 (2013).
10. Mantelli, F. & Argüeso, P. Functions of ocular surface mucins in health and disease. *Curr. Opin. Allergy Clin. Immunol.* **8**, 477–483 (2008).
11. Hoorens, P. R. *et al.* Genome wide analysis of the bovine mucin genes and their gastrointestinal transcription profile. *BMC Genomics* **12**, 140 (2011).
12. Hansson, G. C. Mucins and the microbiome. *Annu. Rev. Biochem.* **89**, 769–793 (2020).

13. Wan, F. *et al.* Lipid shell-enveloped polymeric nanoparticles with high integrity of lipid shells improve mucus penetration and interaction with cystic fibrosis-related bacterial biofilms. *ACS Appl. Mater. Interfaces* **10**, 10678–10687 (2018).
14. Marxen, E., Mosgaard, M. D., Pedersen, A. M. L. & Jacobsen, J. Mucin dispersions as a model for the oromucosal mucus layer in in vitro and ex vivo buccal permeability studies of small molecules. *Eur. J. Pharmaceut. Biopharmaceut.* **121**, 121–128 (2017).
15. Meng-Lund, E., Muff-Westergaard, C., Sander, C., Madelung, P. & Jacobsen, J. A mechanistic based approach for enhancing buccal mucoadhesion of chitosan. *Int. J. Pharm.* **461**, 280–285 (2014).
16. Stie, M. B. *et al.* Swelling of mucoadhesive electrospun chitosan/polyethylene oxide nanofibers facilitates adhesion to the sublingual mucosa. *Carbohydr. Polym.* **242**, 116428 (2020).
17. Völler, M. *et al.* An optimized protocol for assessment of sputum macrorheology in health and muco-obstructive lung disease. *Front. Physiol.* **13**, 19 (2022).
18. Sandberg, T., Blom, H. & Caldwell, K. D. Potential use of mucins as biomaterial coatings. I. Fractionation, characterization, and model adsorption of bovine, porcine, and human mucins. *J. Biomed. Mater. Res. A* **91A**, 762–772 (2009).
19. Collado-González, M., González Espinosa, Y. & Goycoolea, F. M. Interaction between chitosan and mucin: Fundamentals and applications. *Biomimetics* **4**, 32 (2019).
20. Efremova, N. V., Huang, Y., Peppas, N. A. & Leckband, D. E. Direct measurement of interactions between tethered poly(ethylene glycol) chains and adsorbed mucin layers. *Langmuir* **18**, 836–845 (2002).
21. Madsen, J. B. *et al.* Structural and mechanical properties of thin films of bovine submaxillary mucin versus porcine gastric mucin on a hydrophobic surface in aqueous solutions. *Langmuir* **32**, 9687–9696 (2016).
22. Znamenskaya Falk, Y., Engblom, J., Pedersen, J. S., Arnebrant, T. & Kocherbitov, V. Effects of hydration on structure and phase behavior of pig gastric mucin elucidated by SAXS. *J. Phys. Chem. B* **122**, 7539–7546 (2018).
23. Beaucage, G. Small-angle scattering from polymeric mass fractals of arbitrary mass-fractal dimension. *J. Appl. Crystallogr.* **29**, 134–146 (1996).
24. Sogias, I. A., Williams, A. C. & Khutoryanskiy, V. V. Why is chitosan mucoadhesive?. *Biomacromolecules* **9**, 1837–1842 (2008).
25. Szilágyi, B. Á., Mammadova, A., Gyarmati, B. & Szilágyi, A. Mucoadhesive interactions between synthetic polyaspartamides and porcine gastric mucin on the colloid size scale. *Colloids Surf. B Biointerfaces* **194**, 111219 (2020).
26. Thongborisute, J. & Takeuchi, H. Evaluation of mucoadhesiveness of polymers by BIACORE method and mucin-particle method. *Int. J. Pharm.* **354**, 204–209 (2008).
27. Klemetsrud, T., Jonassen, H., Hiorth, M., Kjøniksen, A.-L. & Smistad, G. Studies on pectin-coated liposomes and their interaction with mucin. *Colloids Surf. B Biointerfaces* **103**, 158–165 (2013).
28. Lundin, M., Sandberg, T., Caldwell, K. D. & Blomberg, E. Comparison of the adsorption kinetics and surface arrangement of "as received" and purified bovine submaxillary gland mucin (BSM) on hydrophilic surfaces. *J. Colloid Interface Sci.* **336**, 30–39 (2009).
29. Albarkah, Y. A., Green, R. J. & Khutoryanskiy, V. V. Probing the mucoadhesive interactions between porcine gastric mucin and some water-soluble polymers. *Macromol. Biosci.* **15**, 1546–1553 (2015).
30. Oh, S., Wilcox, M., Pearson, J. P. & Borrós, S. Optimal design for studying mucoadhesive polymers interaction with gastric mucin using a quartz crystal microbalance with dissipation (QCM-D): Comparison of two different mucin origins. *Eur. J. Pharmaceut. Biopharmaceut.* **96**, 477–483 (2015).
31. Mazzarino, L., Coche-Guérente, L., Lemos-Senna, P. L. E. & Borsali, R. On the mucoadhesive properties of chitosan-coated polycaprolactone nanoparticles loaded with curcumin using quartz crystal microbalance with dissipation monitoring. *J. Biomed. Nanotechnol.* **10**, 787–794 (2014).
32. Feiler, A. A., Sahlholm, A., Sandberg, T. & Caldwell, K. D. Adsorption and viscoelastic properties of fractionated mucin (BSM) and bovine serum albumin (BSA) studied with quartz crystal microbalance (QCM-D). *J. Colloid Interface Sci.* **315**, 475–481 (2007).
33. Hopkins, J. B., Gillilan, R. E. & Skou, S. BioXTAS RAW: Improvements to a free open-source program for small-angle X-ray scattering data reduction and analysis. *J. Appl. Crystallogr.* **50**, 1545–1553 (2017).

Acknowledgements

Asger Halfdan Grønborg-Jensen and Adrian Gjetnes Rossebø are thanked for assisting with the preliminary experiments prior to the data included in this work. The authors acknowledge the Novo Nordisk Foundation (BioDelivery; Grand Challenge Programme NNF16OC0021948), Lundbeck Foundation (project no. R303-2018-2968), and VILLUM FONDEN (project no. 19175) for funding this research, and the University of Copenhagen, small-angle X-ray facility, CPHSAXS, funded by the Novo Nordisk Foundation (grant no. NNF19OC0055857).

Author contributions

Mai Bay Stie: Conceptualization, Formal analysis, Investigation, Methodology, Project administration, Roles/Writing-original draft. Cristiana Cunha: Conceptualization, Formal analysis, Investigation, Methodology, Writing-review and editing. Zheng Huang: Investigation, Writing-review and editing. Jacob Judas Kain Kirkensgaard: Methodology, Formal analysis, Writing-review and editing. Pernille Sønderby Tuelung: Methodology, Formal analysis, Writing-review and editing. Feng Wan: Conceptualization, Methodology, Writing-review and editing. Hanne Mørck Nielsen: Conceptualization, Funding acquisition, Methodology, Writing-review and editing. Vito Foderà: Conceptualization, Funding acquisition, Methodology, Writing-review and editing. Stine Rønholt: Conceptualization, Funding acquisition, Formal analysis, Investigation, Methodology, Project administration, Writing-review and editing.

Competing interests

The authors declare no competing interests.

Additional information

Correspondence and requests for materials should be addressed to M.B.S. or S.R.